



Towards the use of dynamic growing seasons in a chemical transport model

A. Sakalli¹ and D. Simpson^{1,2}

¹Dept. Earth & Space Sciences, Chalmers Univ. Technology, Gothenburg, Sweden

²EMEP MSC-W, Norwegian Meteorological Institute, Oslo, Norway

Correspondence to: D. Simpson (david.simpson@met.no)

Received: 17 July 2012 – Published in Biogeosciences Discuss.: 11 September 2012

Revised: 22 November 2012 – Accepted: 23 November 2012 – Published: 14 December 2012

Abstract. Chemical transport models (CTMs), used for the prediction of, for example, nitrogen deposition or air quality changes, require estimates of the growing season of plants for a number of reasons. Typically, the growing seasons are defined in a very simplified way in CTMs, using fixed dates or simple functions. In order to explore the importance of more realistic growing season estimates, we have developed a new and simple method (the T5 method) for calculating the start of the growing season (SGS) of birch (which we use as a surrogate for deciduous trees), suitable for use in CTMs and other modelling systems. We developed the T5 method from observations, and here we compare with these and other methodologies, and show that with just two parameters T5 captures well the spatial variation in SGS across Europe.

We use the EMEP MSC-W chemical transport model to illustrate the importance of improved SGS estimates for ozone and two metrics associated with ozone damage to vegetation. This study shows that although inclusion of more realistic growing seasons has only small effects on annual average concentrations of pollutants such as ozone, the metrics associated with vegetation risk from ozone are significantly affected.

This work demonstrates a strong need to include more realistic treatments of growing seasons in CTMs. The method used here could also be suitable for other types of models that require information on vegetation cover, such as meteorological and regional climate models. In future work, the T5 and other methods will be further evaluated for other forest species, as well as for agricultural and grassland land covers, which are important for emissions and deposition of reactive nitrogen compounds.

1 Introduction

For forest trees, the start of the growing season (SGS) is associated with changes in key biogeochemical processes such as photosynthesis, transpiration and especially CO₂ uptake. The growing season is usually determined by environmental factors, including air and/or soil temperature, daylight length, precipitation and altitude (Mahall et al., 2010; Pinto et al., 2011).

In particular, SGS is highly sensitive to temperature (Polgar and Primack, 2011; Rybski et al., 2011; Doi and Katano, 2008), and hence to the effects of climate change. Several studies have shown the impact of climate change on SGS and the end of the growing season (EGS), for example Menzel and Fabian (1999); Menzel et al. (2006); Penuelas et al. (2009) and Wiedinmyer et al. (2004). Menzel and Fabian (1999) reported that the average annual growing season has extended by almost 11 days since the early 1960s. Chmielewski and Rotzer (2001) reported that the warming in early spring in the last 30 yr caused an earlier start of growing season by 8 days. Further, Myeni et al. (1997) published the effect of seasonality of start of growing season on seasonality of CO₂ in the atmosphere.

A number of different types of models try to predict, or require information on, SGS. These studies include ecosystem models such as the Lund-Potsdam-Jena (LPJ) family of codes (Sykes et al., 1996; Smith et al., 2001), which simulate the growth of vegetation on multi-annual time scales, often on global scales. The LPJ-GUESS version of this code (Smith et al., 2001) has also been used in combination with regional climate models (Smith et al., 2011), and for the estimation of emissions of “biogenic” volatile organic

compounds (BVOCs) such as isoprene or monoterpenes from vegetation (Arneeth et al., 2007; Schurgers et al., 2009).

Chemical transport models (CTMs), which are used to predict concentrations of air pollutants such as ozone or particulate matter, or to predict depositions of e.g. sulphur and nitrogen, also require assumptions about SGS and EGS for dealing with biosphere–atmosphere interactions. Of particular interest for this study, the CTM (Simpson et al., 2012) of the European Monitoring and Evaluation Programme, Meteorological Centre-West (EMEP MSC-W, www.emep.int), requires SGS and EGS for many important processes. These include calculations of the dry deposition of pollutants, including oxidised and reduced nitrogen (Simpson et al., 2006), and for emissions of biogenic volatile organic compounds (BVOCs), which are important for ozone and organic aerosol (Simpson, 1995; Simpson et al., 1999, 2007; Bergström et al., 2012).

The EMEP model is important for the development of policy in Europe, as results from the model underpin the integrated assessment approach, which has been the basis for protocols developed under the United Nation Economic Commission for Europe for more than 30 yr (Sliggers and Kakebeeke, 2004), and within the European Union's Clean Air for Europe programme (Amann et al., 2011). The model has also been used recently to help untangle the connections between nitrogen deposition and forest carbon sequestration (Sutton et al., 2008).

Similarly, numerical weather prediction (NWP) models and general climate models (GCMs) use SGS in their predictions of water and heat fluxes, again often using very simplified treatments of vegetation and growing seasons. For example, the weather research and forecasting (WRF) model (Skamarock and Klemp, 2008) is a well-regarded meso-scale NWP model, widely used also in air quality modelling (e.g. Grell et al., 2005; Zhang, 2008; Foley et al., 2010; Vieno et al., 2010; Zhang, 2008). Vegetation characteristics are mainly prescribed by the input of monthly fields of leaf area index, implying no year-to-year variation. As another example, a revised land surface model (TESSEL), which is implemented in the European Centre for Medium-Range Weather Forecasts (ECMWF) model, uses a constant day (e.g. 26 March) for the start of the growing season for surface exchange over land (Wipfler et al., 2011).

There are several models that calculate SGS as a function of air temperature. The most common approaches use the so-called **growing day degree** (GDD) method, based on daily average temperature to predict SGS (e.g. Smith et al., 2001; Villordon et al., 2009; Wang, 1960). GDD is defined as the number of temperature degrees above a certain threshold base temperature and, as well as SGS, is often used to predict other phenological features such as flowering time (Linkosalo et al., 2008, 2010) or the start of pollen production (Galán et al., 2001; Linkosalo et al., 2010; Sofiev et al., 2012).

Other models use NDVI (**n**ormalized **d**ifferenced **v**egetation **i**ndex) from satellite data to define the start and

end of growing seasons (e.g. Steltzer and Post, 2009; Going Dao-Yi, 2003; Guenther et al., 2006; Cox, 2001; Myeni et al., 1997).

As will be discussed in more detail in Sect. 2.1, the EMEP MSC-W model uses a latitude equation to model SGS and EGS. This simplified method has actually been found to work quite well compared to more complex methods (Tuovinen et al., 2009), but has obvious deficiencies. Not least, it pays no regard to year-to-year variations and cannot account for the differences between locations at the same latitude, but with different climates. This methodology is obviously not ideal for looking at long-term (e.g. decadal or 100 yr) trends of air pollution, especially when linked to expected climate change impacts. In order to improve the ability of the EMEP model to capture year-to-year variations in SGS and EGS, we have tested several methodologies and developed a new dynamic method that depends only on daily average temperature.

This work should be seen as a first step to including more realistic growing seasons in the EMEP model, with the introduction of a meteorological-dependent SGS being compared to the assumption used up to now that SGS is a function of latitude only. To make the modelling of the start of growing season as simple as possible, but still valuable, we chose a species (birch, *B. pubescens*) whose SGS mainly depends on temperature (Körner and Basler, 2010). Beech and oak are other characteristic species for a temperate deciduous forest (Allabay, 2006; Skjøth et al., 2008), which we had considered for this study, but SGS for these species is complicated by a greater dependence on light conditions (Körner and Basler, 2010). However, differences in SGS between different deciduous species are not so great. For example, Menzel et al. (2008) investigated the extension of the growing season in two European countries, and amongst other results they found differences in leaf unfolding of about ± 2 weeks. Even where larger deviations are found (e.g. for alder), there seem to be good correlations between phenological events at the start of the growing season among different species (Linkosalo, 1999).

In this study, we have postulated some simple temperature-dependent equations and compared these and a few other methods for calculating SGS against observed data. We also compare some existing EGS methods to observations. We also investigate the sensitivity of the EMEP CTM model results to the choice of method, in order to quantify the impacts of changes in growing season on a few illustrative metrics of air quality.

There are several different definitions for SGS, including start of budburst (Duchemin et al., 1999), start of leaf unfolding (Beck et al., 2007; Kross et al., 2011; O'Connor et al., 2012), or cambial growth after winter dormancy (Krepkowski et al., 2011; Jyske et al., 2012), and it is often unclear which definition is used in different studies. In this study, we define SGS as the start time of leaf unfolding by the plants.

2 Methods for SGS and EGS

In this paper we compare SGS values calculated using four different methods, and EGS values with two methods. One method will use monthly average temperatures, typical of ecosystem usage, and two will use daily temperatures, from EMEP MSC-W input fields. Sections 2.1–2.4 below describe the methods used. In principal daily temperatures are of course more realistic, but in practice many ecosystem models and other models have to rely upon archived monthly data, and typically daily temperature values are generated using interpolation between these monthly values. In particular, many models (including LPJ-GUESS) make use of the CRU (Climatic Research Unit) climate database. The database provides long-term monthly average temperatures gridded at 0.5° longitude/latitude resolution for the period 1901–2009, and has thus proved an invaluable resource for vegetation modelling.

Figure 1 illustrates the differences inherent in using temperature from an NWP model or from monthly CRU data. The averages of the NWP method (monthly values not shown) and the CRU data are actually quite close, especially in the first half of the year, but the day-to-day change in temperature is of course much more variable using direct daily NWP data. Interestingly, this figure shows several examples where daily average temperatures from the NWP model exceed 5°C , a threshold that is often used alone to define growing seasons. Using interpolated data from monthly averages, this 5°C would only be exceeded after about 3 months, but in the NWP data the first exceedances occur in January.

2.1 “LAT” method

The LAT method is the default latitude-based method of the EMEP model. The calculation of SGS and EGS in the EMEP model is a function of latitude, not climate. The equations used are

$$d_{\text{SGS, LAT}} = d_{\text{SGS, 50}} + \Delta_{\text{SGS}} (\phi - 50) \quad (1)$$

where $d_{\text{SGS, LAT}}$ is the ordinal day of SGS, $d_{\text{SGS, 50}}$ ($= 100$ for deciduous trees) defines the start of the growing season at 50°N , ϕ is latitude in degrees, and Δ_{SGS} is the increase in SGS per degree N, set as 1.5 days/degree for deciduous trees. For the end of the growing season, we use

$$d_{\text{EGS, LAT}} = d_{\text{EGS, 50}} + \Delta_{\text{EGS}} (\phi - 50) \quad (2)$$

where $d_{\text{EGS, 50}}$ and Δ_{EGS} define the end of the growing season in an analogous way to the SGS terms.

These equations were loosely developed to fit data presented in Zhang et al. (2004), although modified in consultation with European forest experts from the UNECE “mapping manual” process (LRTAP, 2010). These equations have been found to fit a wide range of data (Emberson, 2009), and have often been found to perform better than more complex methods (see e.g. Tuovinen et al., 2009).

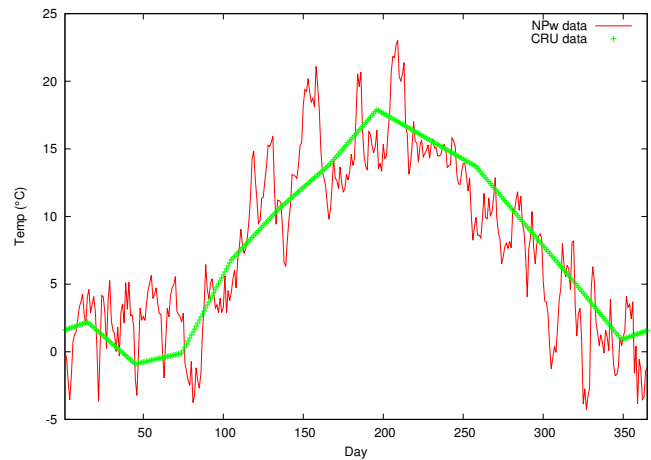


Fig. 1. The daily average temperature from the ECMWF numerical weather prediction model (as input to the EMEP model) and as interpolated from the CRU climate database for a low-altitude location in northern Germany.

2.2 “LPJ-CRU” method

LPJ-GUESS is an object-oriented, modular framework to model the dynamics of ecosystem structure and functioning from the patch scale to the global scale (Smith et al., 2001). Standard LPJ-GUESS uses the CRU climate database as noted above. In default usage, the daily average temperatures are approximated by using interpolation functions to estimate daily temperatures from these monthly average data. These estimated daily temperatures are then used for the calculation of growing degree days (GDD). A detailed documentation of the interpolation function is found in Smith et al. (2001). In the model from Smith et al. (2011), the growing degree days to budburst (GDD^0) are first calculated as a function of the length of the chilling period (Sykes et al., 1996):

$$\text{GDD}^0 = a + b \cdot e^{-k \cdot C}, \quad (3)$$

where C is the number of days over the winter period¹ with the temperature $< 5^\circ\text{C}$ (chilling days) and a , b and k are species-specific constants (for *Betula pubescens* $a = 0$, $b = 350$ and $k = 0.05$). The growing degree days until a specific ordinal day j are calculated with

$$\text{GDD}_{5, \text{LPJ}}^j = \sum_{i=1}^{i=j} \max(0, T_i - 5) \quad (4)$$

where T_i is the daily average temperature in $^\circ\text{C}$ on day i , and the max function returns the value $T_i - 5$ where $T_i > 5$, otherwise zero. The SGS is then calculated with

$$d_{\text{SGS, LPJ}} = \text{First day } i \text{ where } \text{GDD}_{5, \text{LPJ}}^i > \text{GDD}^0. \quad (5)$$

¹As defined in the LPJ-GUESS code, chilling days start to be accumulated once the running 31-day average temperature in autumn/winter drops below 5°C .

The modelling of EGS begins after the start of growing season in a location. First we calculate the sum of daily fractional leaf cover (equivalent number of days with full leaf cover) so far this growing season:

$$A_{LPJ}^j = \sum_{i=d_{SGS,LPJ}}^{i=j} \min\left(1, \frac{GDD_{5,LPJ}^i - GDD_0}{\Delta GDD_5}\right), \quad (6)$$

where ΔGDD_5 (= 200) is the the GDD needed on 5 °C base to attain full leaf cover. EGS is then calculated as

$$d_{EGS,LPJ} = \text{First day } i, \text{ after } d_{SGS,LPJ}, \text{ where } A_{LPJ}^i > A_{LPJ}^{\max} \quad (7)$$

where A_{LPJ}^{\max} (= 210) is the maximum number of equivalent days with full leaf cover per growing season.

2.3 “TTM” method

The thermal time model (TTM) was developed by Linkosalo et al. (2010) and calibrated by Sofiev et al. (2012) for Europe using data from Siljamo et al. (2008) and data from the European Aerobiological Network (EAN, <https://ean.polleninfo.eu/Ean/>), to calculate leaf budburst for birch. The calculation of SGS using TTM begins with a modified heat sum:

$$GDD_{3.5,TTM}^j = \sum_{i=t_0}^{i=j} \max(T_i - T_{crit}, 0) \quad (8)$$

where $GDD_{3.5,TTM}^j$ is this modified heat sum ($H(t)$ in the notation of Sofiev et al., 2012), t_0 the first day of counting ($t_0 = 60$, ~ 1 March, as in Sofiev et al., 2012), and T_{crit} is the critical temperature threshold (3.5 °C). Sofiev et al. (2012) used the TTM to predict onset and duration of flowering. In this work, we assume that the start of flowering and start of leaf budburst are quite close, usually a reasonable assumption within some days uncertainty (Linkosalo, 1999), and calculate our SGS using the same criteria as Sofiev et al. used for flowering:

$$d_{SGS,TTM} = \text{First day } i \text{ where } GDD_{3.5,TTM}^i > H_{fs}. \quad (9)$$

H_{fs} is a temperature sum threshold for the start of the season, which varies by location. We used maps of H_{fs} calculated by Sofiev et al. (2012) (as available at <http://silam.fmi.fi/MACC/>).

Sofiev et al. (2012) also present methods of calculating the end of the pollen season, but this is physiologically different to the EGS required in this work, so we use TTM only for SGS calculations.

2.4 “T5” method

A new method tested here was designed to make use of one simple parameter, near-surface temperature from the NWP model, but accounting for geographical differences in plant response.

The T5 method considers that plants in warm regions need more days in which the daily average temperature is continuously more than 5 °C than in cold regions. This is loosely consistent with the assumption that the heat sum requirement in warm regions is greater than in cold regions (cf. Sofiev et al., 2012), and with experimental results that the number of the days needed to budburst is often related to the number of chilling days (which is usually related to the duration of winter). For example, Myking and Heide (1995) and Myking (1999) found that the days to budburst for *Betula pendula* Roth and *B. pubescens* seedlings decreased with increased duration of chilling.

Thus, we assume that birch needs a particular time range in which the daily average temperature is always more than 5 °C to start unfolding of leaves, and that this time range is shorter in colder conditions. We have developed the following two equations to express this dependency:

$$D_{u,i} = \alpha - \beta i \quad (10)$$

$$d_{SGS,T5} = \text{First day } i \text{ where all } T_{i-D_{u,i}} \cdots T_i \geq 5^\circ\text{C} \quad (11)$$

where $D_{u,i}$ is the required number of days for the start of the unfolding of the leaves for a given ordinal day i , α (= 39) and β (= 0.2) are empirical constants, and SGS is defined as the first day where a number, $D_{u,i}$, of previous days have daily average temperatures exceeding 5 °C. We test Eqs. (10)–(11) for all days i starting at $i = 1$ until Eq. (11) is satisfied. Figure 2 illustrates how $D_{u,i}$ varies with day number. The parameter values ($\alpha = 39$, $\beta = 0.2$) in Eq. (10) were found by optimising against the observed SGS data, in terms of regression slope and correlation coefficient, using meteorological data from the year 2008. The index of agreement and mean absolute error discussed below were not part of the optimisation. This procedure is further commented on in Sect. 5.1.

As an example of usage, to end up with $d_{SGS,T5}$ around day 100, we have $D_{u,100} = 19$, so temperatures must have been $\geq 5^\circ\text{C}$ from days 81 to 100. For much colder regions, where we ended up with say $d_{SGS,T5} = 180$, then $D_{u,100} = 3$, so only days 178–180 above 5 °C were needed before the growing season is assumed to start.

The T5 methodology is deliberately simple, but it has a number of advantages:

- A single temperature threshold is used across Europe, but the methodology accounts in a natural way for the differences between cold and warm climates, with plants in e.g. northern Europe (or at high altitude) requiring only a few days with temperatures exceeding 5 °C, whereas plants in warmer areas require longer periods of warmth before growth starts.
- The methodology is self-consistent and can be applied for any model resolution and is not dependent on external data (e.g. no specification of heat-sum thresholds is needed).

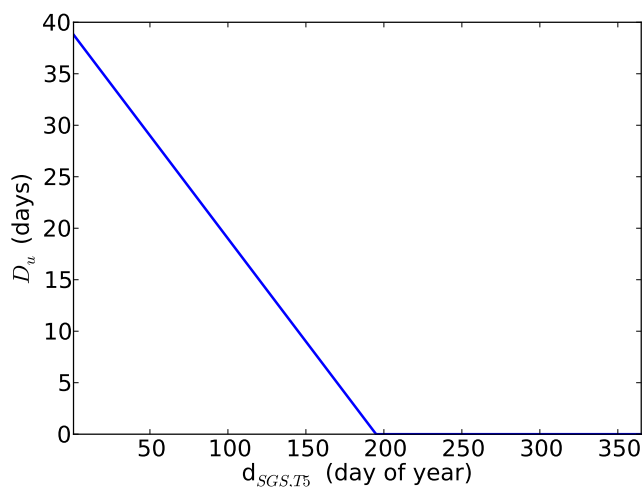


Fig. 2. The required number of days to start leaf unfolding by birch as a function of the start of growing season.

- SGS can be calculated from current-year temperature fields only; it avoids the need for data from previous winters for example.

Of course, the methodology has disadvantages too. It does not explicitly account for chilling events and is less sophisticated than methods such as those of Myking and Heide (1995) and Hanninen (1990). The species (birch) for which this method is developed and tested has simpler requirements for leaves and flowering than other species (e.g. alder, Linkosalo, 1999; oak or beech, Körner and Basler, 2010). The methodology is empirical, rather than biologically based, and thus cannot account for many aspects of climate change (this is discussed further in Sect. 6). However, we will show that the methodology can be quite successful in reproducing the spatial variation in SGS for birch seen across Europe, and thus it serves as a useful first step to improving the treatment of growing seasons in the EMEP model. This also allows us to explore the importance of more accurate estimates of growing season for some air quality indicators associated with biosphere–atmosphere exchange.

3 Observations and statistical approach

To develop the T5 method, and evaluate this and other SGS and EGS methods described above, we compare with the PAN European Phenological Database (PEP) (PAN, 2011). The PEP database includes observation data from 31 European countries and has in total collected data from 18 687 stations.

We found 2029 observed data records from 122 stations in 23 European countries around the start of the growing season for *B. pubescens*. Most observation stations (77 of 122) are located in Finland, Germany and the Netherlands. The data records for SGS were mostly taken between 1971 and 1991,

but records up to 2009 were available at some sites. The earliest observed SGS values were day 56 in the Netherlands, and the latest day 175 in Finland. Most stations (107 of 122) are located below 500 m above sea level. The highest station is located at 1550 m a.s.l. in Greece. For the end of the growing season (EGS), we found suitable datasets at 55 stations. Table 1 summarises the available data for SGS, and Table 2 provides details of SGS for each location.

In Sect. 5.1 we will present comparisons between the estimated and observed SGS and EGS. However, two important complications in making this comparison are (i) differences in the altitude of the observed SGS and modelled temperature data, and (ii) differences in the years available for comparison.

The effect of altitude on temperature and the vegetation has been reported in the many studies (e.g. Beals, 1969; Caprio, 1993; Klimes, 2003; Luo et al., 2004; Korner, 2007). A 100 m increase in altitude causes a temperature decline of about 0.6 °C. In principal we could account for this, but the NWP and CRU data are also applicable to a given altitude, and their interpretation is problematic. For example, the NWP data input to the EMEP model is provided in terrain-following coordinates, for grid cells of ca. 50 km × 50 km in extent. The NWP model's near-surface temperature is in some senses a temperature applicable to an average terrain height, but at the same time it has been derived through assumptions applicable only to flat homogeneous terrain. In order to avoid some of the problems that are inevitably introduced when comparing data in mountain regions, we restrict our analysis to sites where the difference in the NWP model's (or CRU data) terrain height and the observation site is within 100 m.

Direct year-to-year comparison between observed SGS, EGS and estimated values is also problematic. Most observed SGS and EGS values were recorded between 1971 and 1994. In a few locations, the SGS data were observed between 2005 and 2009. We have daily ECMWF NWP data from the EMEP system available only for 2005 onwards. It was therefore not possible to make a comparison of the observed SGS and modelled SGS year by year except over a very limited data range. The CRU data could have been used in principal, but as discussed above, the use of interpolated data from monthly records can be misleading when comparing to daily temperature thresholds, and we are primarily seeking a method for use with CTMs that can make use of detailed temperature data. Therefore we calculated the average SGS of each station and compared with average modelled SGS for 5 yr. This approach ignores therefore year-to-year variability at particular stations, and indeed the effects of climate trends, but is aimed at capturing the larger geographical differences that the PAN database provides.

However, for 23 stations we were able to compare estimates of average SGS from all the data with average SGS from 2005–2009 values (where at least three of these years were available), and the differences were found to be rather

Table 1. Summary of the observation stations with data records for SGS in the PAN database. Note that countries can have several stations, taking observations for different years.

Country	Number Sites	Number Obs.	Years	Range in SGS (days)	Altitude range (m a.s.l.)
AT	3	50	1971–1999	79–134	150–900
BA	1	21	1971–1991	104–143	1000
BE	2	46	1971–1997	79–135	15–500
CH	1	29	1971–2000	90–122	600
DE	22	482	1971–2000	80–166	13–1370
DK	4	49	1971–1994	92–135	5–40
FI	37	693	1971–2009	113–175	5–335
FR	1	9	1978–1988	91–135	70
GR	1	9	1973–1982	110–125	1550
HR	2	35	1971–2000	74–118	64–146
HU	2	21	1974–1994	90–134	90–220
IT	5	135	1968–2009	63–129	14–80
ME	1	18	1975–1993	69–120	5
MR	1	3	1975–1994	98–116	240
NL	18	71	1868–1978	56–125	0–25
NO	5	144	1965–2005	105–144	25–95
PL	2	33	1971–2000	87–128	74–127
PR	1	9	1971–1979	64–95	30
RS	2	37	1975–1993	82–121	90–121
SE	6	32	1971–2007	105–149	33–320
SK	2	58	1971–2000	86–132	180–540
SL	1	29	1971–2000	93–121	310
UK	2	16	1971–2009	88–117	64–84

small. As expected, SGS values from the recent years were somewhat earlier than from the longer-term averages, but by only 3.1 days on average, with a biggest discrepancy of less than eight days.

For each station, we thus extracted the temperature from the NWP and/or CRU climate databases for each year between 2005 and 2009. We will illustrate the comparison between the estimates and observed SGS and EGS. As well as calculating the regression lines, and correlation coefficient between the observed and modelled SGS and EGS, we also calculated the mean absolute error (MAE) and index of agreement, d , (Willmott, 1982) for the validation of the results of the models:

$$\text{MAE} = \frac{1}{n} \sum_{i=1}^n |P_i - O_i| \quad (12)$$

$$d = 1 - \frac{\sum_{i=1}^n (P_i - O_i)^2}{\sum_{i=1}^n ((|P_i - \bar{O}|) + (|O_i - \bar{O}|))^2}, \quad (13)$$

where P is the simulation and O is the observation data, i a particular sample, n the number of samples, overbar representing mean values, and d the index of agreement, respectively.

4 Modelling studies

As noted in Sect. 1, the EMEP MSC-W model is used to provide estimates of a number of pollutants, and metrics associated with health and vegetation effects. Some metrics, such as sulphur and nitrogen deposition, are not expected to be very sensitive to SGS and EGS, since deposition is largely related to emissions, and these are almost entirely from combustion sources. Here we focus on ozone damage indicators that are expected to be sensitive to SGS, since at many sites (especially in northern Europe) ozone concentrations peak in springtime, usually the period where the growing season starts (e.g. Monks, 2000; Karlsson et al., 2007; Scheel et al., 1997). The EMEP model is described briefly in Sect. 4.1 and the selected metrics for this study described in Sect. 4.2. An illustration of the performance of the EMEP model for some selected stations in Europe is given in Fig. 3. This figure illustrates that the EMEP model usually performs well for ozone in very different parts of Europe. It also illustrates the importance of springtime ozone at many of these sites.

In Sect. 5.2 we will illustrate the effect of using a dynamic growing season on these selected metrics, using two runs of the EMEP model. In the “base” run, we run the EMEP model with the standard latitude method for SGS and EGS. In a second test scenario, we run the EMEP model with the

Table 2. Comparison of average observed SGS of *B. pubescens* from the PAN database with estimated SGS using T5, LPJ-CRU, TTM and LAT (EMEP standard) methods.

Lat. (°N)	Long. (°E)	Alt. (m a.s.l.)	SGS Obs.	LAT	LPJ- CRU*	TTM	T5
69.05	27.10	156	160	129	141	173	163
68.40	27.38	301	162	129	139	172	160
68.38	23.65	301	163	129	141	175	162
68.02	24.15	276	157	128	141	168	158
67.73	29.60	321	158	128	141	169	158
67.58	24.20	336	152	128	132	165	154
67.35	23.82	161	150	127	132	164	153
67.02	27.25	216	158	126	134	161	150
66.82	28.40	196	143	126	137	162	152
66.35	26.72	154	141	125	128	157	144
66.30	25.00	118	147	125	127	155	143
64.80	26.00	26	140	123	122	148	144
64.52	26.45	116	153	123	122	147	147
64.23	19.77	226	149	122	127	153	147
63.92	23.88	41	141	122	120	142	139
63.55	29.02	143	139	121	122	147	142
63.50	10.87	61	132	121	–	142	133
63.07	29.82	136	138	121	120	147	142
63.07	21.72	6	139	120	120	145	134
63.00	27.72	116	137	121	117	143	141
62.77	30.97	149	138	120	119	147	142
62.73	25.18	161	137	120	117	145	140
62.63	27.05	120	136	120	116	144	141
62.60	29.72	81	137	120	120	148	142
62.07	24.48	136	136	119	114	139	134
62.02	23.03	114	138	119	112	138	133
61.80	29.32	82	135	119	114	146	141
61.38	25.03	121	136	118	113	136	131
61.02	24.45	131	133	118	112	135	131
60.88	14.40	321	142	117	115	138	138
60.62	26.17	31	133	117	110	133	131
60.43	22.75	51	136	117	112	135	131
60.38	22.55	11	133	117	112	135	131
60.05	23.03	16	130	116	111	135	130
59.67	10.78	96	129	116	100	126	124
57.23	9.92	21	121	112	108	116	118
57.17	14.78	181	131	112	91	126	129
55.97	13.33	51	122	110	102	120	124
55.87	12.50	41	125	110	93	116	115
55.67	12.30	31	125	109	92	114	115
54.95	−7.72	61	85	109	89	100	109
53.78	21.58	128	118	107	90	115	125
53.73	9.88	14	105	107	91	105	115
53.67	10.27	51	116	107	88	105	115
53.65	10.20	47	112	107	88	105	115
53.33	−6.23	31	100	106	88	100	109
52.85	6.18	1	113	105	–	99	110
52.75	6.90	1	114	105	94	101	113
52.38	−6.93	81	99	105	–	98	109
52.38	4.63	1	111	105	100	94	100
52.27	5.60	1	125	104	92	98	109
52.25	17.10	75	97	105	84	105	117
52.22	4.63	1	102	104	–	96	109
52.20	5.97	1	109	104	92	98	109
52.20	13.20	43	103	104	82	101	113

Table 2. Continued.

Lat. (°N)	Long. (°E)	Alt. (m a.s.l.)	SGS Obs.	LAT	LPJ- CRU*	TTM	T5
52.10	5.12	1	102	104	91	96	109
52.00	5.97	1	93	104	92	97	103
51.98	5.67	26	108	104	90	97	103
51.97	7.63	61	106	104	93	100	114
51.97	6.22	1	109	104	96	98	109
51.95	6.47	1	110	104	96	98	109
51.80	5.40	1	97	104	89	97	103
51.73	5.13	1	115	103	89	96	103
51.57	5.07	1	86	103	92	96	103
51.48	3.95	1	111	103	91	94	101
51.32	3.62	1	105	103	91	92	103
51.28	3.43	1	117	103	93	91	78
51.08	−0.88	85	107	103	95	95	101
50.98	3.80	16	104	103	92	92	103
50.98	13.53	361	117	103	86	106	118
50.00	5.73	501	113	101	90	109	112
49.77	7.05	481	109	100	85	107	112
49.75	6.67	266	103	101	86	104	110
49.02	−0.03	71	123	100	95	88	100
48.82	9.12	331	105	99	79	100	110
48.72	9.22	381	108	99	79	100	110
48.45	18.93	541	113	99	–	108	112
48.40	11.73	461	114	99	85	104	116
48.33	18.37	181	114	98	80	97	107
48.25	16.72	151	101	98	81	95	108
48.25	16.37	203	100	98	80	95	108
48.18	11.17	541	119	98	82	107	116
48.07	7.68	266	106	98	79	91	108
47.95	8.52	681	118	98	–	110	118
47.60	19.35	221	106	97	79	94	103
47.33	21.13	91	100	97	75	91	101
46.03	16.57	147	105	95	75	89	104
45.78	19.12	91	98	95	75	85	99
44.37	20.95	122	101	93	–	84	103
43.75	18.02	1001	125	92	92	113	120

Notes: * “–” indicates no values, due to complications with land/sea overlap and/or topography.

T5 method for the modelling of SGS, preserving the standard EMEP method for EGS.

4.1 The EMEP MSC-W model

The EMEP MSC-W chemical transport model used in this work (Simpson et al., 2012) is a development of the 3-D CTM of Berge and Jakobsen (1998), extended with photo-oxidant and inorganic aerosol chemistry. The model domain used in this study covers the whole of Europe, and includes a large part of the North Atlantic and Arctic areas. The standard grid system of the EMEP model is based on a polar stereographic projection, with a horizontal resolution of 50 km × 50 km at latitude 60°. The model includes 20 vertical layers, using terrain-following coordinates, and the lowest layer has a thickness of about 90 m.

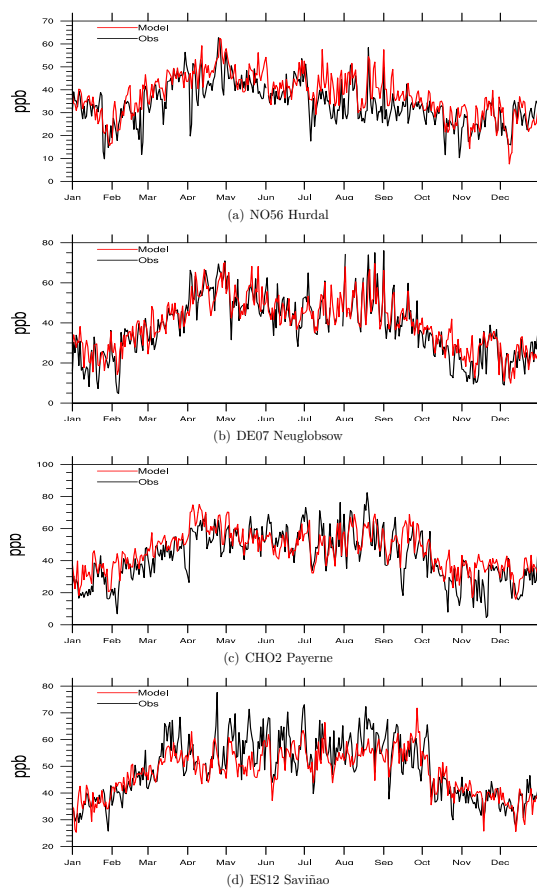


Fig. 3. Comparison of modelled and observed daily maximum ozone (ppb) values at four European sites in 2009: **(a)** Hurdal, Norway (NO56), **(b)** Neuglobsow, Germany (DE07), **(c)** Payerne, Switzerland (CH02) and **(d)** O Saviñao, Spain (ES12).

The model is capable of using various meteorological data inputs, but in standard use and here we use meteorological fields derived from the European Centre for Medium-Range Weather Forecasting Integrated Forecasting System (ECMWF-IFS) model (<http://www.ecmwf.int/research/ifsdocs/>). These data have 3-hourly resolution, and include the near-surface (2 m) temperature (T_2) that we will use in this study.

In the standard EMEP MSC-W model (Simpson et al., 2012; S12 for section and equation references to follow), SGS and EGS are specified as simple functions of latitude for different land cover classes (S12: Sect. 5, Table 3). These SGS values are used to derive leaf area indices (LAIs), which control emissions of BVOCs (S12: Sect. 6.6, Eq. (22); see also Sect. 4). The LAI amount, and timing of SGS, also influences the dry deposition (and hence ozone uptake calculations) through direct LAI impacts on surface resistances (S12: Sect. 8, Eq. 55), through light and phenology factors involved in the stomatal conductance calculations (S12: Eq. 57), non-stomatal resistances (S12: Eq. 60), and aerosol

deposition rates (S12: Eq. 69). The timing of SGS also influences soil-NO emissions (S12: Eq. 24) and dust emissions (S12: Sect. 6.10), although these SGS effects are only used for agricultural lands.

Evaluation of the EMEP model's performance for ozone concentrations has been presented elsewhere (e.g. Jonson et al., 2006; Colette et al., 2011; or for many individual sites for the year 2009, Gauss et al., 2011). Examining results from 43 EMEP sites included in the present runs, we found mean overpredictions of daily maximum ozone of ca. 5 % for the winter (DJF) months, ca. 6 % for spring (MAM), 8 % for summer (JJA), and ca. 14 % for the autumn months (SON). Model performance changes considerably from site to site, however, and the reasons for this are often not so clear: likely sometimes model-related, sometimes problems with the observations. The issue of EMEP model performance with respect to the ozone uptake parameters is even more difficult, but has been tackled in several previous papers (e.g. Tuovinen et al., 2001, 2004, 2007, 2009 and Klingberg et al., 2008).

As noted in Sect. 1, the EMEP model is one of the key tools in the development of air pollution emissions policy in Europe. The model has to be not only state of the art in terms of model performance when compared to measurements, but also very efficient in computer processing in order to conduct literally thousands of scenario runs. This means that modelling of pollution transfer between the atmosphere and biosphere needs to be simple enough to ensure reasonable model run times, yet complex enough to incorporate the key drivers of for example O_3 or nitrogen deposition fluxes at the European scale. The application of the model across such a large spatial region also means that the complexity of the model has to be balanced against the availability of spatial data characterising the important physical and environmental conditions that will influence for example ozone concentrations or nitrogen deposition across Europe (e.g. land cover, species distribution, soil type, root depth and meteorological information).

4.2 Model outputs

Some specific outputs of the EMEP model are of interest for this work. Firstly, we have two metrics commonly used to indicate risks of ozone damage to vegetation in Europe: AOT40 and POD_1 . These metrics have been described in detail elsewhere (LRTAP, 2010), but are briefly summarised here.

(i) POD_Y

Phyto-toxic ozone dose is the accumulated stomatal ozone flux over a threshold Y $\text{nmole } O_3 \text{ m}^{-2} \text{ s}^{-1}$:

$$POD_Y = \int \max(F_{st} - Y, 0) dt \quad (14)$$

where the stomatal flux, F_{st} , and threshold, Y , are in $\text{nmole } O_3 \text{ m}^{-2} \text{ s}^{-1}$ (per projected leaf area). This integral is

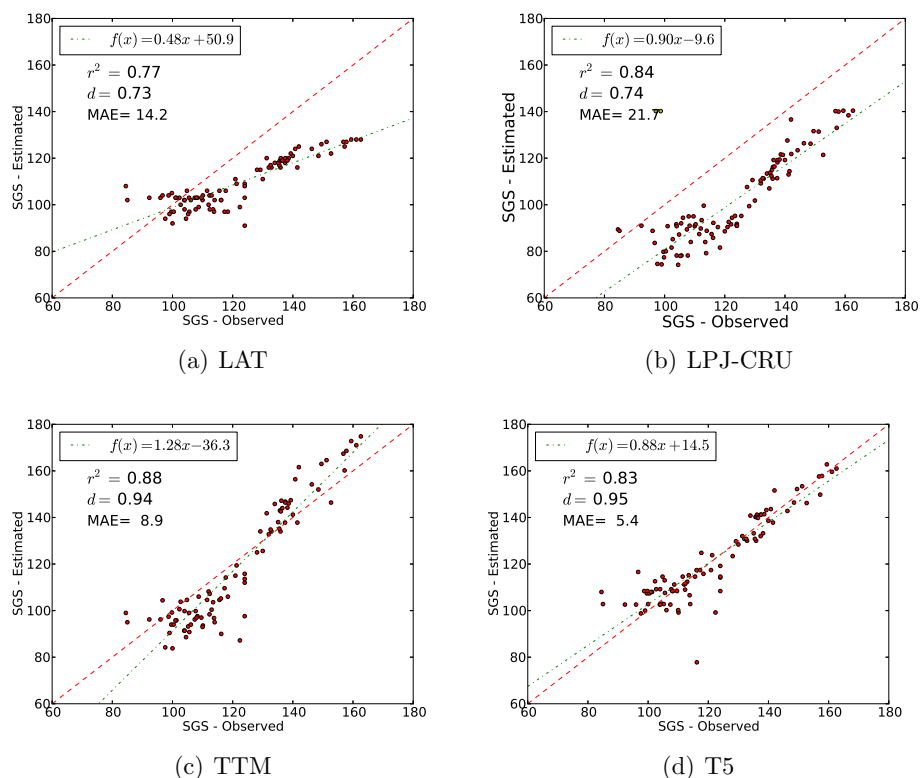


Fig. 4. Comparison of estimated and observed SGS (day number) using the methods LAT, LPJ-CRU, TTM and T5. The regression and 1:1 lines are also indicated, along with correlation coefficient (r), mean absolute error (MAE) and index of agreement (d). For LPJ-CRU two stations (marked in yellow, near observed SGS 98, estimated 140) are obvious outliers and have been excluded from the statistics.

evaluated over time, from the start of the growing season (SGS) to the end (EGS). The flux F_{st} is calculated using the so-called DO₃SE model (Emberson et al., 2000, 2001; Simpson et al., 2001, 2003; Tuovinen et al., 2009). Details of the method and parameters have changed over the years, but the latest version is documented in Simpson et al. (2012).

(ii) AOT40

AOT40 is the accumulated amount of ozone over the threshold value of 40 ppb:

$$\text{AOT40} = \int \max(\text{O}_3 - 40 \text{ ppb}, 0) dt. \quad (15)$$

This integral is also taken over time, namely the relevant growing season for the vegetation concerned. The corresponding unit is ppb hours (abbreviated to ppb h). The usage and definitions of AOT40 have changed over the years though, and with different applications. Here we use AOT40 calculated from ozone values at the top of the canopy, during daylight hours, consistent with mapping manual recommendations (LRTAP, 2010).

In recent effects work, POD-type metrics are clearly preferred over AOT40 for forest and crop species, but we present AOT40 here as the definition is conceptually simpler than

POD, and AOT40 is still relevant for semi-natural vegetation (LRTAP, 2010). AOT40 is also rather similar to the so-called SOMO35 metric, which is recommended as the relevant ozone indicator by WHO (2004). SOMO35 is calculated as the sum over the year of the daily 8-h maximum ozone concentrations in excess of a 35 ppb threshold. The POD metric was previously denoted $\text{AF}_{st}Y$ (accumulated stomatal flux over threshold Y) and has been compared to AOT40 over Europe by Simpson et al. (2007).

Our third metric is the annual average concentration of ozone, primarily in order to compare with the two effect metrics above, which are based upon O₃. Also, ozone is a key oxidant in tropospheric chemical cycles (Monks et al., 2009), an important greenhouse gas, and highly coupled to carbon sequestration (e.g. Sitch et al., 2007).

5 Results

5.1 Evaluation of SGS and EGS methods

Figure 4 compares the SGS predictions of the four SGS methods (Sect. 2) against observed values from the PAN database. Actual values are given in Table 2 (as noted in Sect. 2, we restrict our analysis to situations where the

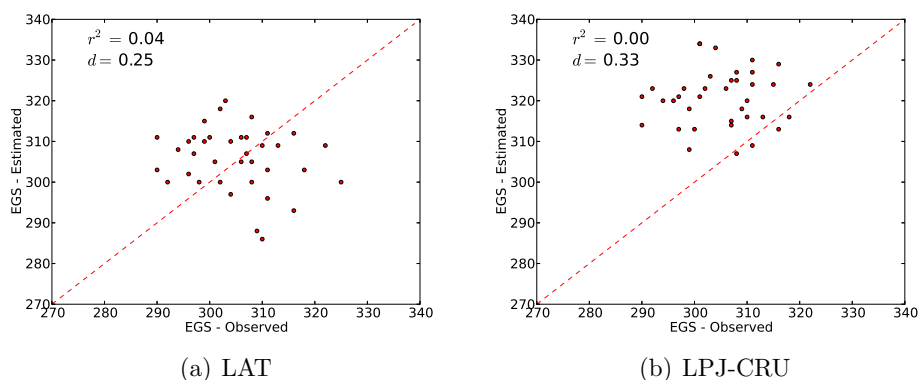


Fig. 5. Comparison of observed and estimated EGS (day number) using the methods LAT (=EMEP default) and LPJ-CRU at stations from the PAN database. Regression lines are not given since neither method shows significant correlation with the data.

difference in the NWP model's terrain height and the observation site is within 100 m). The regression line, 1 : 1 line, correlation coefficients (r^2), mean absolute error (MAE), and index of agreement (d) are also given on these plots.

The r^2 values range between 77 % to 88 %, indicating quite good performance for all methods. The very simple LAT method correlates quite well with the observations ($r^2 = 0.77$), but the regression line has a slope of just 0.48, and large intercept of 51 days. The modelled SGS with the LAT method covers a much smaller range of values than the observed. The poorest index of agreement is found for the LPJ-CRU method ($d = 0.74$), which uses monthly average temperature, but the correlation ($r^2 = 0.84$) is much better than the LAT method. There is a clear tendency for the method to predict SGS values earlier than the measurements, with the largest MAE of about 22 days. This difference compared to the other models is likely due to the fact that LPJ-GUESS is designed for global-scale usage, whereas the other methods were optimised for European application (further, in the LPJ-GUESS model the development of birch leaves at the start of the season extends over a long period, which will partly compensate for this early start of SGS). The TTM method performs well with this dataset, with $r^2 = 0.88$ and $d = 0.94$, although with a slope of 1.28 and quite large (36-day) intercept. Mean absolute error is within 9 days. TTM is thus significantly better than the default latitude method.

Finally, the simple T5 method performs rather well, with the best index of agreement ($d = 0.95$), lowest MAE (5.4 days), and a regression line that is almost coincident with the 1 : 1 line (Fig. 4(d)). The correlation coefficient ($r^2 = 0.83$) is not so high as with LPJ-CRU or TTM, but still good. The scatter in this plot is significantly larger when the observed SGS is lower than about day 125. Examination of the spatial distribution of these data (Supplement, Fig. S1) shows that discrepancies between the T5 methodology and the observations are generally associated with proximity to the coast, for example at all the Irish sites, and at a site in northern France. This may well stem from the temperature data being used;

grid cells with mixed sea and land areas can easily have unrepresentative temperatures. The very good agreement (low scatter) for days with SGS > 125 is associated with Nordic sites, but Fig. S1 also shows that the T5 method gives consistently good results across much of Europe. Of course, much of this good agreement stems from the fact that the parameters of the T5 method were obtained by fitting this dataset (optimising for r^2 and slope), but this fitting was done for 1 yr of meteorology only, whereas here we use results from five meteorological years. The fact that all three statistical measures fit so well suggests that the underlying model has a good structure (we have also tested the use of a simpler model with fixed values for the $D_{u,i}$ parameter; results were not as good, however; see Supplement, Fig. S2).

Figure 5 compares EGS estimates from the two available methods with observations. It is clearly seen that both methods perform poorly in reproducing observed EGS values. The range of observed EGS is quite small, with most values between days 290–320, suggesting that factors other than temperature control this phase of the growing season. It could be said that the EMEP model's current assumption of a latitude-dependent (and hence, implicitly, photoperiod-dependent) EGS is no worse than the more physiologically based LPJ methods. This would be partly consistent with Partanen et al. (1998) who suggested that the day length and photoperiod could be the drivers for leaf colouring and end of growing season in boreal and temperate environments. However, one could also argue for a simpler fixed-date system (at least in preference to the methods tried here), since the correlation is essentially zero for both methods.

5.2 EMEP model simulations

As discussed in Sect. 4.2, we have selected three outputs from the EMEP model to illustrate the importance of variations in SGS and EGS: the two ozone effects – metrics $POD_{1,DF}$ and $AOT40_{DF}$ – and annual mean ozone concentration.

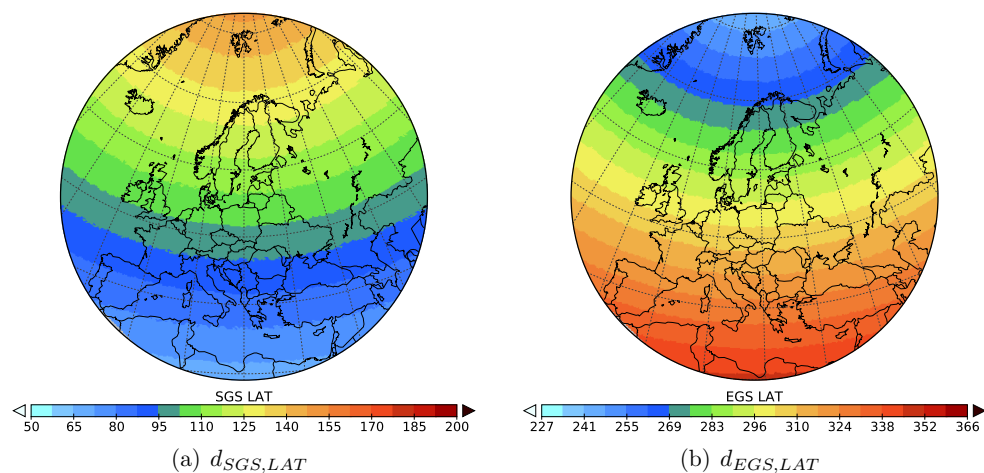


Fig. 6. Estimated start and end of growing season in Eurasia, using the standard EMEP LAT method.

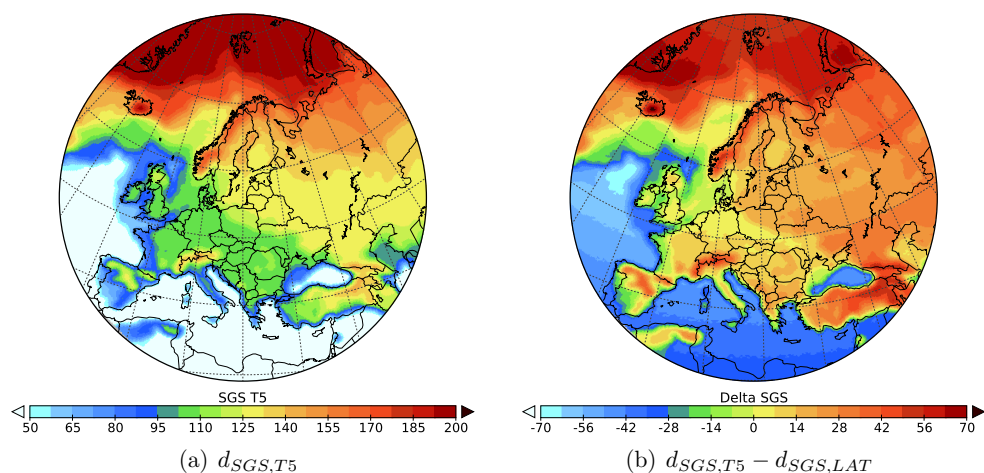


Fig. 7. (a) Estimated start of the growing season using the T5 method, and (b) the difference between the T5 and LAT methods.

We have run the EMEP model using the two growing season methods (LAT and T5) and taken the difference between the scenarios to find out the effect of the changing of the growing season on the four output metrics. Figures 6 and 7 illustrate the estimated distribution of SGS and EGS obtained using the EMEP LAT method, and SGS as estimated by the T5 method. The T5 SGS values are obviously much more complex than those obtained with the LAT method, reflecting both climate differences across Europe and topographic effects. Fig. 7b shows significant differences between the two methods, with T5 SGS values frequently more than a month later than the LAT values (e.g. in the Alps, western Norway, Turkey).

Figure 8 shows the modelled $\text{POD}_{1,\text{DF}}$ across Eurasia when using the LAT method for the year 2009. Highest values, of around 30 mmole m^{-2} , are found in southern Europe, but values exceed 10 mmole m^{-2} over much of the continent (for comparison, Mills et al., 2011 recommended critical lev-

els of 4 mmole m^{-2} for birch and beech forests; although our generic deciduous forest class is not strictly comparable, the values seen in Fig. 8 suggest extensive areas at risk of ozone).

Figure 8b shows the difference in modelled $\text{POD}_{1,\text{DF}}$ when using the T5 methodology. The effect of the different SGS methods is different in different parts of Europe. In many parts of southern Europe, $\text{POD}_{1,\text{DF}}$ using the T5 method is significantly higher than in the base case run (LAT). In other parts, especially northern and eastern Europe, and mountain areas, $\text{POD}_{1,\text{DF}}$ with T5 is lower than in the base case. These changes are as expected: delayed SGS means less exposure to the spring peak in ozone in many parts of Europe. Changes are of the order of $2\text{--}5 \text{ mmole m}^{-2}$, corresponding to about 10 % of the base values in many areas.

The modelled values of $\text{AOT}_{40,\text{DF}}$ are illustrated in Fig. 9a. As shown and discussed already in Simpson et al. (2007), modelled AOT40 values show much stronger gradients than

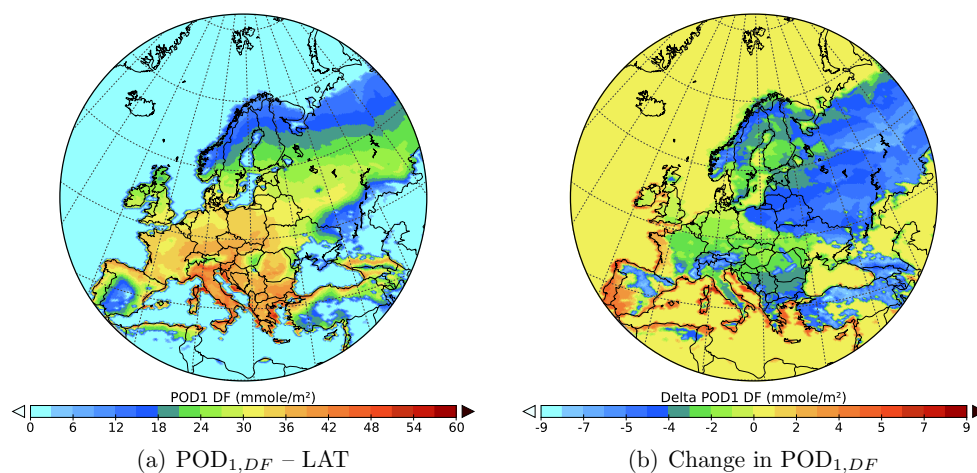


Fig. 8. Modelled values of (a) $POD_{1,DF}$ (mmole m^{-2}) using the EMEP LAT method, and (b) the difference (T5 minus LAT) in modelled $POD_{1,DF}$ when using the T5 method. Calculations for 2009.

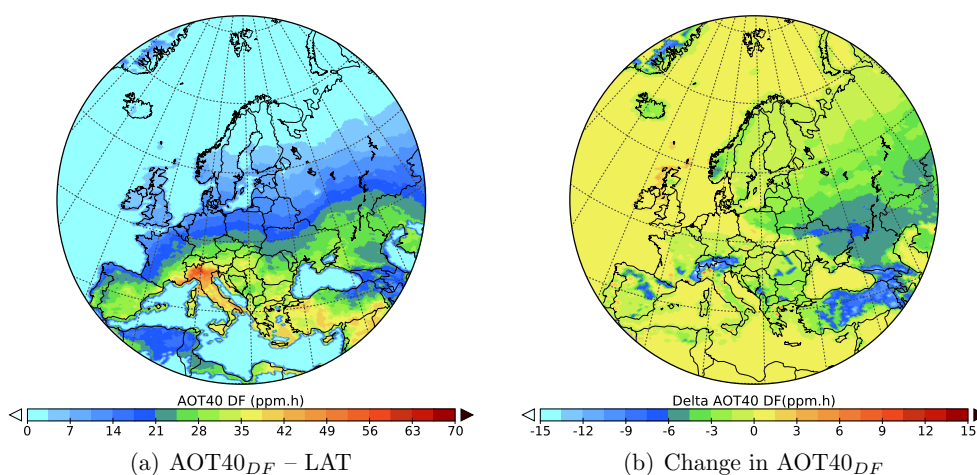


Fig. 9. Modelled values of (a) $AOT_{40,DF}$ (units: ppm h) using the EMEP LAT method, and (b) the difference (T5 minus LAT) in modelled $AOT_{40,DF}$ when using the T5 method. Calculations for 2009.

those of the flux indicator $POD_{1,DF}$. Highest values (over 40 000 ppb h) are seen in the Alps and northern Italy.

The implementation of the T5 method lowers $AOT_{40,DF}$ in many parts of Europe, with largest changes of ca. 10 000 ppb h in mountain areas. This method leads to moderate increases in parts of the United Kingdom, Denmark, in eastern France and also in some regions in southern Europe. Elsewhere (e.g. over much of central and eastern Europe) changes are much smaller, typically with T5 leading to reductions in $AOT_{40,DF}$ of around 1–2000 ppb h , about 10 % of the values given by the LAT method.

The predictions of surface annual average O_3 concentrations using the EMEP standard model and the effect of implementation of the T5 method on the surface O_3 concentrations are shown in Fig. 10. The distribution of ozone reflects well-known patterns, with a general north–south gradi-

ent (e.g. Scheel et al., 1997), and higher levels over sea areas where ozone deposition is very low. The gradients in ozone are also much smaller than those of $AOT_{40,DF}$ or $POD_{1,DF}$, a result of the thresholds used in these ozone metrics, which amplify the importance of the higher end of the ozone (or ozone flux) frequency distributions (Tuovinen et al., 2007; Sofiev and Tuovinen, 2001).

Figure 10 shows that the impact of the changing SGS values is quite small on mean ozone levels, with changes being smaller than 0.5 ppb almost everywhere. This finding is illustrated further in Fig. 11, which shows daily maximum ozone concentrations (at canopy top) and daily $POD_{1,DF}$ values for two sites (in Greece and Sweden), using the base case (LAT) SGS estimates and the T5 estimates. The use of the T5 SGS values is seen to have very little effect on O_3 itself (see discussion in Sect. 6) but a rather significant effect on the

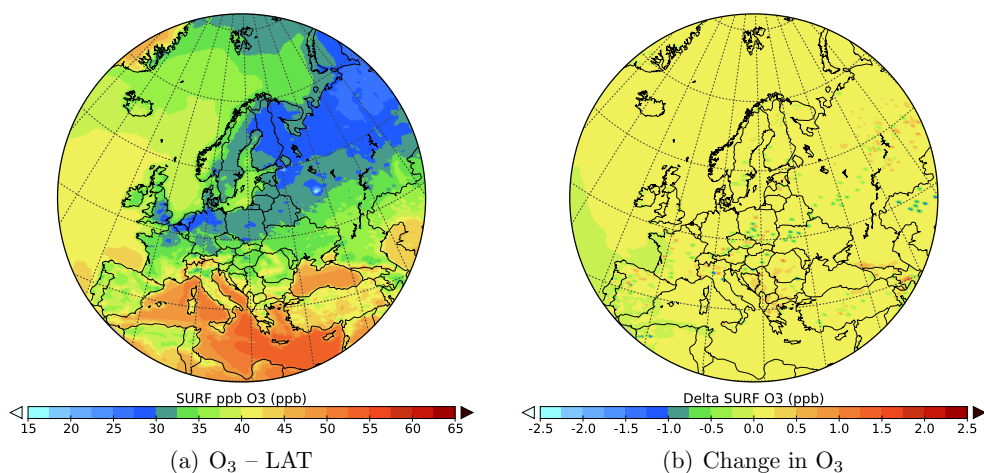


Fig. 10. Modelled values of (a) annual average O_3 concentration (units: ppb) using the EMEP LAT method, and (b) the difference (T5 minus LAT) in modelled O_3 concentration when using the T5 method. Calculations for 2009.

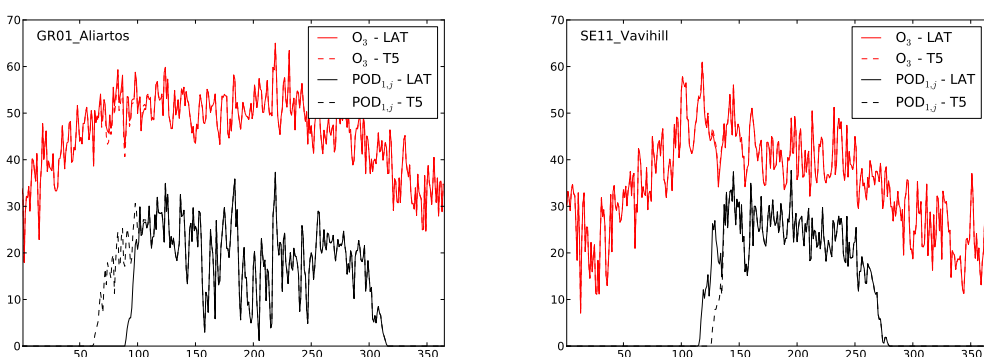


Fig. 11. Calculated daily maximum ozone concentrations (at canopy top, units: ppb) for 2009, and daily $POD_{1,DF}$ values (units: mmole m^{-2}), for sites in Greece (left) and Sweden (right), using the base case (LAT) SGS estimates and the T5 estimates.

length of the growing season, and therefore on the accumulated POD values.

Finally, we have explored the response of other outputs of the EMEP model to this change in SGS, but such responses are generally very small. For example, use of the T5 method instead of LAT produces changes in the modelled fields of nitrogen dry deposition of up to a few mg(N) m^{-2} , less than one percent of the base case deposition values of several hundred mg(N) m^{-2} (see e.g. Simpson et al., 2006).

6 Discussion

As discussed above, the use of the T5 methodology as introduced here results in differences in SGS of deciduous forests (DF) of typically 10–30 days in many parts of Europe, sometimes more (cf. Fig. 7), with the SGS generally delayed compared to that of the default EMEP LAT method. The results of the EMEP model simulations discussed in Sect. 5.2 show that differences in SGS estimates can have significant effects on the two ozone metrics $POD_{1,DF}$ and $AOT_{40,DF}$. On the

other hand, the annual average ozone concentration itself was shown to be very insensitive to these SGS changes. Other metrics such as nitrogen deposition were also found to be very insensitive to these SGS changes.

There are several reasons for these strong differences in response. Firstly, it is important to remember that here we change SGS only for deciduous forests. Thus, growing seasons are unchanged for coniferous forests, crops, grasslands, semi-natural and all other land cover classes in the EMEP model. The $POD_{1,DF}$ and $AOT_{40,DF}$ metrics are directly linked to deciduous forests, whereas most other metrics (e.g. ozone concentrations) are under the influence of all land cover categories.

Further, ozone concentrations frequently show peaks in springtime (Monks, 2000; Karlsson et al., 2007; Scheel et al., 1997) (see also Fig. 3). Metrics such as $AOT_{40,DF}$ and $POD_{1,DF}$ are accumulated over a relatively short time period, which is defined by SGS and EGS, and shifts in this time period can significantly affect the accumulated ozone exposure or dose.

Other metrics are rather insensitive to vegetation characteristics in this springtime period. For example, those aspects of biosphere–atmosphere exchange that most affect ozone are deposition processes and biogenic VOC (BVOC) emissions. Ozone deposition occurs to all vegetative canopies, so a change in just DF only affects a fraction of the total deposition. Further, in springtime much of ozone deposition is through the non-stomatal rather than stomatal pathways (Fowler et al., 2009), and even stomatal fluxes are quite low until temperatures rise well above 5 °C, so emergence of leaves has only a limited impact on the total deposition sink. Biogenic VOC are also strongly temperature dependent (Guenther et al., 2006), so again changes in leaf area at the beginning of the growing season have only a limited effect (at least with existing parameterisations; recent work on BVOC emissions has also suggested that flowering rather than pure temperature control may result in high emissions during springtime; Baghi et al., 2012).

The small sensitivity of the modelled nitrogen deposition to the SGS changes shares some of these features. In this case, the non-stomatal contributions to deposition are even larger than for ozone (e.g. Burkhardt et al., 2009; Flechard et al., 2011; Fowler et al., 2009; Sutton et al., 2007), and to a large extent the deposition of nitrogen has to match the emissions input – and in Europe most emissions of reactive nitrogen are from anthropogenic combustion sources.

The performance of both tested methods for EGS was rather poor. Certainly, temperature alone is not driving EGS, and other factors such as light have an important role. This clearly warrants more study but likely requires more advanced modelling frameworks. On the other hand, it is probably more important to establish the start rather than the end of the growing season, not least as ozone concentrations are usually higher near SGS than near EGS. There are also studies suggesting that ozone uptake at the start of the growing season is more important than towards the end (Pääkkönen et al., 1996; Ashmore, 2005, and references cited therein).

As noted in the Introduction, the work presented here is seen as a first step towards quantifying the importance of using improved growing seasons in CTMs, and we chose a species (birch) that allowed an approach based purely upon temperature. Plant phenology is however a complex issue, and in most species many other factors also influence or control SGS and EGS. Such factors will need to be accounted for in climate change evaluations (Körner and Basler, 2010). Accounting for these will certainly require more complex methods, and likely better links to ecosystem models such as LPJ-GUESS; indeed, this is our long-term aim for the EMEP MSC-W model. So, although LPJ-GUESS here did not capture SGS as well as the “tuned” European empirical methods, an improved calibration would likely produce better results, and such models will almost certainly be required in the future. These models are also developing rapidly in terms of their ability to handle individual species (e.g. Hickler et al., 2012).

A natural extension of this work will be to evaluate the T5 and other methodologies for other forest species, and other land use categories, including those associated with agriculture. Further work is needed to explore the extent to which dynamic SGS values over other vegetation canopies might affect biosphere–atmosphere exchange in this case. For example, emissions and deposition of oxidised and reduced nitrogen compounds from agricultural areas depend on the growing seasons of for example crops and pastures (e.g. Fowler et al., 2009; Skjøth et al., 2011). Indeed, the timing of key agricultural activities is linked to local knowledge of growing seasons. This influences for example fertiliser application and cutting times, which can strongly influence biosphere–atmosphere exchange of NH₃ (e.g. Loubet et al., 2002).

7 Conclusions

In order to explore the importance of using more realistic growing season estimates in chemical transport models, we have developed a new and simple method (the T5 method) for calculating the start of the growing season (SGS) of birch (which we use as a surrogate for deciduous trees). This method is intended as a first step to the introduction of dynamic growing seasons in the EMEP MSC-W chemical transport model. Although clearly more testing is needed for a broader range of species, the simple requirements of the T5 method might make it suitable for use in other CTMs and other modelling systems.

The T5 method is empirical, based upon a simple equation with just two free parameters. We show that with this formulation a very good fit to the observed SGS values for birch is attained, in terms of the regression statistics, mean absolute error, and index of agreement.

We developed the T5 method with observations from the PAN European Phenological Database, which provided appropriate data from 122 stations for SGS (and 55 for EGS). We also compared this with the simple latitude-based scheme currently used in the EMEP MSC-W model, the LPJ-GUESS scheme using monthly CRU data, and with the Finnish thermal time system, which is used for pollen modelling. All methods performed quite well for the start of the growing season, especially those developed specifically for Europe (TTM and T5) and driven by daily meteorological data. The LPJ-GUESS code, driven by monthly data, also gave good correlation but predicted SGS too early compared to the other methods (this is partly compensated in the LPJ-GUESS code by a long development time for LAI for birch, but may also reflect that LPJ-GUESS has a more global focus than the other methods; parameters are not optimised for European conditions). For the end of the growing season, the two available methods performed poorly, but uncertainties about the end of the growing season are probably less important than those for SGS.

The SGS values generated by T5 can be significantly different from those of the simple default latitude function used in the EMEP model, with differences of 10–30 days over many parts of Europe. The T5 values present a much more realistic picture of the variation of SGS across Europe.

We have used the EMEP MSC-W chemical transport to illustrate the importance of improved SGS estimates for ozone and two metrics associated with ozone damage to vegetation. This study shows that although inclusion of more realistic growing seasons has only small effects on annual average concentrations of pollutants such as ozone, the metrics associated with vegetation risk from ozone are significantly affected. The ozone flux metric, $POD_{1,DF}$, decreased in most areas of Europe, showing largest decreases at high latitudes (e.g. Scandinavia, northern Russia) or at high elevations (e.g. the Alps). Although these areas have quite low base-case POD values, the levels are still appreciable and likely damaging for vegetation, and many of these areas are also heavily forested. On the other hand, $POD_{1,DF}$ levels are increased in some areas (e.g. Portugal and the west coast of France) by ca. 3–5 $mmole\ m^{-2}$, and these areas were already experiencing some of the highest $POD_{1,DF}$ values in the base case.

In this study, the impacts of a dynamic SGS applied to deciduous forests on other long-term pollution metrics such as nitrogen deposition are small. We have presented a number of reasons for this, but an important need is to explore the impact of improved SGS for other types of vegetation, including agriculture. This work demonstrates a strong need to include more realistic treatments of growing seasons in CTMs.

Supplementary material related to this article is available online at: <http://www.biogeosciences.net/9/5161/2012/bg-9-5161-2012-supplement.pdf>.

Acknowledgements. This study was supported by the Swedish Strategic Research Area project, MERGE – Modelling the Regional and Global Earth system, and by the EU projects ECLAIRE (project no: 282910), and PEGASOS (265148) as well as EMEP under UNECE. Thanks are due to Ben Smith, Paul Miller and colleagues at Lund University for the provision of the LPJ-GUESS code and help in its implementation. Thanks are also due to Birthe Marie Steensen at the Norwegian Meteorological Institute in Oslo for help with the TTM methodology.

Edited by: S. Reis

References

- Allabay, M.: Temperate Forests (Biomes of the Earth), Chelsea House Publications, 2006.
- Amann, M., Bertok, I., Borcken-Kleefeld, J., Cofala, J., Heyes, C., Hoeglund-Isaksson, L., Klimont, Z., Nguyen, B., Posch, M., Rafaj, P., Sandler, R., Schoepp, W., Wagner, F., and Winiwarer, W.: Cost-effective control of air quality and greenhouse gases in Europe: Modeling and policy applications, *Environ. Model. Softw.*, 26, 1489–1501, doi:10.1016/j.envsoft.2011.07.012, 2011.
- Arneth, A., Niinemets, Ü., Pressley, S., Bäck, J., Hari, P., Karl, T., Noe, S., Prentice, I. C., Serça, D., Hickler, T., Wolf, A., and Smith, B.: Process-based estimates of terrestrial ecosystem isoprene emissions: incorporating the effects of a direct CO_2 -isoprene interaction, *Atmos. Chem. Phys.*, 7, 31–53, doi:10.5194/acp-7-31-2007, 2007.
- Ashmore, M.: Assessing the Future Global Impacts of Ozone on Vegetation, *Plant, Cell and Environment*, 28, 949–964, 2005.
- Baghi, R., Helmig, D., Guenther, A., Duhl, T., and Daly, R.: Contribution of flowering trees to urban atmospheric biogenic volatile organic compound emissions, *Biogeosciences*, 9, 3777–3785, doi:10.5194/bg-9-3777-2012, 2012.
- Beals, E. W.: Vegetation change along altitudinal gradients, *Science*, 165, 981–985, 1969.
- Beck, P. S. A., Jonsson, P., Hogda, K.-A., Karlsen, S. R., Eklundh, L., and Skidmore, A. K.: A ground-validated NDVI dataset for monitoring vegetation dynamics and mapping phenology in Fennoscandia and the Kola peninsula, *Int. J. Remote Sens.*, 28, 4311–4330, doi:10.1080/01431160701241936, 2007.
- Berge, E. and Jakobsen, H. A.: A regional scale multi-layer model for the calculation of long-term transport and deposition of air pollution in Europe, *Tellus*, 50, 205–223, 1998.
- Bergström, R., Denier van der Gon, H. A. C., Prévôt, A. S. H., Yttri, K. E., and Simpson, D.: Modelling of organic aerosols over Europe (2002–2007) using a volatility basis set (VBS) framework: application of different assumptions regarding the formation of secondary organic aerosol, *Atmos. Chem. Phys.*, 12, 8499–8527, doi:10.5194/acp-12-8499-2012, 2012.
- Burkhardt, J., Flechard, C. R., Gresens, F., Mattsson, M., Jongejan, P. A. C., Erisman, J. W., Weidinger, T., Meszaros, R., Nemitz, E., and Sutton, M. A.: Modelling the dynamic chemical interactions of atmospheric ammonia with leaf surface wetness in a managed grassland canopy, *Biogeosciences*, 6, 67–84, doi:10.5194/bg-6-67-2009, 2009.
- Caprio, J. M.: Flowering Dates, Potential Evapotranspiration and Water-use Efficiency of *Syringa-vulgaris* L At Different Elevations In the Western United-states-of-america, *Agr. Forest Meteorol.*, 63, 55–71, doi:10.1016/0168-1923(93)90022-A, 1993.
- Chmielewski, F. M. and Rotzer, T.: Response of tree phenology to climate change across Europe, *Agr. Forest Meteorol.*, 108, 101–112, doi:10.1016/S0168-1923(01)00233-7, 2001.
- Colette, A., Granier, C., Hodnebrog, Ø., Jakobs, H., Maurizi, A., Nyiri, A., Bessagnet, B., D'Angiola, A., D'Isidoro, M., Gauss, M., Meleux, F., Memmesheimer, M., Mieville, A., Rouil, L., Russo, F., Solberg, S., Stordal, F., and Tampieri, F.: Air quality trends in Europe over the past decade: a first multi-model assessment, *Atmos. Chem. Phys.*, 11, 11657–11678, doi:10.5194/acp-11-11657-2011, 2011.

- Cox, P.: Description of the “TRIFFID” dynamic global model, Tech. rep., Handley Centre, 2001.
- Doi, H. and Katano, I.: Phenological timings of leaf budburst with climate change in Japan, *Agr. Forest Meteorol.*, 148, 512–516, doi:10.1016/j.agrformet.2007.10.002, 2008.
- Duchemin, B., Goubier, J., and Courrier, G.: Monitoring phenological key stages and cycle duration of temperate deciduous forest ecosystems with NOAA/AVHRR data, *Remote Sens. Environ.*, 67, 68–82, doi:10.1016/S0034-4257(98)00067-4, 1999.
- Emberson, L., Simpson, D., Tuovinen, J. P., Ashmore, M. R., and Cambridge, H. M.: Towards a model of ozone deposition and stomatal uptake over Europe. 6/2000 EMEP MSC-W Note, The Norwegian Meteorological Institute, Oslo, Norway, 2000
- Emberson, L. D., Ashmore, M. R., Simpson, D., Tuovinen, J. P., and Cambridge, H. M.: Modelling and mapping ozone deposition in Europe, *Water Air Soil Pollut.*, 130, 577–582, 2001
- Emberson, L.: Development and application of methods for modelling and mapping ozone deposition and stomatal flux in Europe, Annual/interim project report to UK Dept. for Environ., Food and Rural Affairs, project AW0601PP, Stockholm Environment Institute at York, UK, 2009.
- Flechar, C. R., Nemitz, E., Smith, R. I., Fowler, D., Vermeulen, A. T., Bleeker, A., Erisman, J. W., Simpson, D., Zhang, L., Tang, Y. S., and Sutton, M. A.: Dry deposition of reactive nitrogen to European ecosystems: a comparison of inferential models across the NitroEurope network, *Atmos. Chem. Phys.*, 11, 2703–2728, doi:10.5194/acp-11-2703-2011, 2011.
- Foley, K. M., Roselle, S. J., Appel, K. W., Bhave, P. V., Pleim, J. E., Otte, T. L., Mathur, R., Sarwar, G., Young, J. O., Gilliam, R. C., Nolte, C. G., Kelly, J. T., Gilliland, A. B., and Bash, J. O.: Incremental testing of the Community Multiscale Air Quality (CMAQ) modeling system version 4.7, *Geosci. Model Dev.*, 3, 205–226, doi:10.5194/gmd-3-205-2010, 2010.
- Fowler, D., Pilegaard, K., Sutton, M. A., Ambus, P., Raivonen, M., Duyzer, J., D. Simpson, D., Fagerli, H., Fuzzi, S., Schjoerring, J. K., Granier, C., Neftel, A., Isaksen, I. S. A., Laj, P. Maione, M., Monks, P. S., Burkhardt, J., Daemmgen, U., Neiryneck, J., Personne, E., Wichink-Kruit, R., Butterbach-Bahl, K., Flechar, C., Tuovinen, J. P., Coyle, M., Gerosa, G., Loubet, B., Altimir, N., Gruenhage, L., Ammann, C., Cieslik, S., Paoletti, E., Mikkelsen, T. N., Ro-Poulsen, H., Cellier, P., Cape, J. N., Horváth, L., Loreto, F., Niinemets, Ü., Palmer, P. I., Rinne, J., Misztal, P., Nemitz, E., Nilsson, D., Pryor, S., Gallagher, M. W., Vesala, T., Skiba, U., Brüeggemann, N., Zechmeister-Boltenstern, S., Williams, J., O’Dowd, C., Facchini, M. C., de Leeuw, G., Flossman, A., Chaumerliac, N., and Erisman, J. W.: Atmospheric composition change: Ecosystems-Atmosphere interactions, *Atmos. Environ.*, 43, 5193–5267, 2009
- Galán, C., García-Mozo, H., Cariñanos, P., Alcázar, P., and Domínguez-Vilches, E.: The role of temperature in the onset of the *Olea europaea* L. pollen season in southwestern Spain, *Int. J. Biometeorol.*, 45, 8–12, 2001.
- Gauss, M., Benedictow, A., and Hjellbrekke, A.-G.: Photo-oxidants: validation and combined maps, Supplementary material to emep status report 1/2011, available online at: www.emep.int, The Norwegian Meteorological Institute, Oslo, Norway, 2011.
- Going Dao-Yi, S. P.-J.: Northern hemispheric NDVI variations associated with large-scale climate indices in spring, *Int. J. Remote Sens.*, 24, 2559–2566, 2003.
- Grell, G. A., Peckham, S. E., Schmitz, R., McKeen, S. A., Frost, G., Skamarock, W. C., and Eder, B.: Fully coupled “online” chemistry within the WRF model, *Atmos. Environ.*, 39, 6957–6975, 2005.
- Guenther, A., Karl, T., Harley, P., Wiedinmyer, C., Palmer, P. I., and Geron, C.: Estimates of global terrestrial isoprene emissions using MEGAN (Model of Emissions of Gases and Aerosols from Nature), *Atmos. Chem. Phys.*, 6, 3181–3210, doi:10.5194/acp-6-3181-2006, 2006.
- Hänninen, H.: Modelling bud dormancy release in trees from cool and temperate regions. *Acta Forestalia Fennica*, 213, 1–47, 1990.
- Hickler, T., Vohland, K., Feehan, J., Miller, P. A., Smith, B., Costa, L., Giesecke, T., Fronzek, S., Carter, T. R., Cramer, W., Kuehn, I., and Sykes, M. T.: Projecting the future distribution of European potential natural vegetation zones with a generalized, tree species-based dynamic vegetation model, *Glob. Ecol. Biogeogr.*, 21, 50–63, 2012.
- Jonson, J. E., Simpson, D., Fagerli, H., and Solberg, S.: Can we explain the trends in European ozone levels?, *Atmos. Chem. Phys.*, 6, 51–66, doi:10.5194/acp-6-51-2006, 2006.
- Jyske, T., Manner, M., Makinen, H., Nojd, P., Peltola, H., and Repo, T.: The effects of artificial soil frost on cambial activity and xylem formation in Norway spruce, *Trees-Structure and Function*, 26, 405–419, doi:10.1007/s00468-011-0601-7, 2012.
- Karlsson, P. E., Tang, L., Sundberg, J., Chen, D., Lindskog, A., Pleijel, H.: Increasing risk for negative ozone impacts on vegetation in northern Sweden, *Environ. Poll.*, 150, 96–106, 2007.
- Klimes, L.: Life-forms and clonality of vascular plants along an altitudinal gradient in E Ladakh (NW Himalayas), *Basic and Applied Ecology*, 4, 317–328, doi:10.1078/1439-1791-00163, 2003.
- Klingberg, J., Danielsson, H., Simpson, D., and Pleijel, H.: Comparison of modelled and measured ozone concentrations and meteorology for a site in south-west Sweden: Implications for ozone uptake calculations, *Environ. Poll.*, 115, 99–111, 2008.
- Körner, C.: The use of ‘altitude’ in ecological research, *Trends Ecol. Evol.*, 22, 569–574, doi:10.1016/j.tree.2007.09.006, 2007.
- Körner, C. and Basler, D.: Phenology Under Global Warming, *Science*, 327, 1461, doi:10.1126/science.1186473, 2010
- Kramer, K., Leinonen, I., and Loustau, D.: The importance of phenology for the evaluation of impact of climate change on growth of boreal, temperate and Mediterranean forests ecosystems: an overview, *Int. J. Biometeorol.*, 44, 67–75, doi:10.1007/s004840000066, 2000.
- Krepkowski, J., Braeuning, A., Gebrekirstos, A., and Strobl, S.: Cambial growth dynamics and climatic control of different tree life forms in tropical mountain forest in Ethiopia, *Trees-Structure and function*, 25, 59–70, doi:10.1007/s00468-010-0460-7, 2011.
- Kross, A., Fernandes, R., Seaquist, J., and Beaubien, E.: The effect of the temporal resolution of NDVI data on season onset dates and trends across Canadian broadleaf forests, *Remote Sens. Environ.*, 115, 1564–1575, doi:10.1016/j.rse.2011.02.015, 2011.
- Linkosalo, T.: Regularities and patterns in the spring phenology of some boreal trees, *Silva Fennica*, 33, 237–245, 1999.
- Linkosalo, T., Lappalainen, H. K., and Hari, P.: A comparison of phenological models of leaf bud burst and flowering of boreal trees using independent observations, *Tree Physiol.*, 28, 1873–1882, 2008.
- Linkosalo, T., Ranta, H., Oksanen, A., Siljamo, P., Luomajoki, A., Kukkonen, J., and Sofiev, M.: A double-threshold temperature

- sum model for predicting the flowering duration and relative intensity of *Betula pendula* and *B. pubescens*, *Agr. Forest Meteorol.*, 150, 1579–1584, doi:10.1016/j.agrformet.2010.08.007, 2010.
- Loubet, B., Milford, C., Hill, P. W., Tang, Y. S., Cellier, P., and Sutton, M. A.: Seasonal variability of apoplastic NH_4^+ and pH in an intensively managed grassland. *Plant and Soil*, 238, 97–110, 2002.
- LRTAP: Mapping critical levels for vegetation, in: *Manual on Methodologies and Criteria for Mapping Critical Loads and Levels and Air Pollution Effects, Risks and Trends. Revision of 2010*, edited by: Mills, G., UNECE Convention on Long-range Transboundary Air Pollution, International Cooperative Programme on Effects of Air Pollution on Natural Vegetation and Crops, updated version available at: <http://www.rivm.nl/en/themasites/icpmm>, 2010.
- Luo, T. X., Pan, Y. D., Ouyang, H., Shi, P. L., Luo, J., Yu, Z. L., and Lu, Q.: Leaf area index and net primary productivity along subtropical to alpine gradients in the Tibetan Plateau, *Glob. Ecol. Biogeogr.*, 13, 345–358, doi:10.1111/j.1466-822X.2004.00094.x, 2004.
- Mahall, B. E., Thwing, L. K., and Tyler, C. M.: A quantitative comparison of two extremes in chaparral shrub phenology, *FLORA*, 205, 513–526, doi:10.1016/j.flora.2009.12.011, 2010.
- Menzel, A.: *Phänologie von Waldbäumen unter sich ändernden Klimabedingungen – Auswertung der Beobachtungen in den Internationalen Phäologischen Gärten und Mölichkeiten der Modellierung von Phänodaten*, Universitätsbuchhandlung Heinrich Frank, 1997.
- Menzel, A. and Fabian, P.: Growing season extended in Europe, *Nature*, 397, 659, doi:10.1038/17709, 1999.
- Menzel, A., Sparks, T. H., Estrella, N., Koch, E., Aasa, A., Ahas, R., Alm-Kuebler, K., Bissolli, P., Braslavská, O., Briede, A., Chmielewski, F. M., Crepinsek, Z., Curnel, Y., Dahl, A., Defila, C., Donnelly, A., Filella, Y., Jatca, K., Mage, F., Mestre, A., Nordli, O., Penuelas, J., Pirinen, P., Remisova, V., Scheifinger, H., Striz, M., Susnik, A., Van Vliet, A. J. H., Wielgolaski, F.-E., Zach, S., and Züst, A.: European phenological response to climate change matches the warming pattern, *Glob. Change Biol.*, 12, 1969–1976, doi:10.1111/j.1365-2486.2006.01193.x, 2006.
- Menzel, A., Estrella, N., Heitland, W., Susnik, A., Schleip, C., and Dose, V.: Bayesian analysis of the species-specific lengthening of the growing season in two European countries and the influence of an insect pest, *Int. J. Biometeorol.*, 52, 209–218, 2008.
- Mills, G., Pleijel, H., Braun, S., Büker, P., Bermejo, V., Calvo, E., Danielsson, H., Emberson, L., Grünhage, L., Fernández, I. G., Harmens, H., Hayes, F., Karlsson, P. E., and Simpson, D.: New stomatal flux-based critical levels for ozone effects on vegetation. *Atmos. Environ.*, 45, 5064–5068, 2011.
- Monks, P. S.: A review of the observations and origins of the spring ozone maximum. *Atmos. Environ.*, 34, 3545–3561, 2000.
- Monks, P. S., Granier, C., Fuzzi, S., Stohl, A., Williams, M., Aki-moto, H., Amman, M., Baklanov, A., Baltensperger, U., Bey, I., Blake, N., Blake, R. S., Carslaw, K., Cooper, O. R., Dentener, F., Fowler, D., Fragkou, E., Frost, G., Generoso, S., Ginoux, P., Grewé, V., Guenther, A., Hansson, H. C., Henne, S., Hjorth, J., Hofzumahaus, A., Huntrieser, H., Isaksen, I. S. A., Jenkin, M. E., Kaiser, J., Kanakidou, M., Klimont, Z., Kulmala, M., Laj, P., Lawrence, M. G., Lee, J. D., Lioussé, C., Maione, M., McFiggans, G., Metzger, A., Mieville, A., Moussiopoulos, N., Orlando, J. J., O’Dowd, C., Palmer, P. I., Parrish, D. D., Petzold, A., Platt, U., Poeschl, U., Prévot, A. S. H., Reeves, C. E., Reimann, S., Rudich, Y., Sellegri, K., Steinbrecher, R., Simpson, D., ten Brink, H., Theloke, J., van der Werf, G. R., Vautard, R., Vestreng, V., Vlachokostas, Ch., and von Glasow, R.: Atmospheric Composition Change – Global and Regional Air Quality Atmos. Environ., 43, 5268–5350, 2009.
- Myeni, R. B., Keeling, C. D., Tucker, C. J., Asrar, G., and Nemani, R. R.: Increased plant growth in the northern high latitudes from 1981 and 1991, *Nature*, 386, 699–702, 1997.
- Myking, T. and Heide, O. M.: Dormancy release and chilling requirement of buds of latitudinal ecotypes of *Betula pendula* and *B. pubescens*, *Tree Physiol.*, 15, 697–704, 1995.
- Myking, T.: Winter dormancy release and budburst in *Betula pendula* ROTH and *B. pubescens* EHRH. ecotypes, *Phyton-annales Rei Botanicae*, 39, 139–145, 1999.
- O’Connor, B., Dwyer, E., Cawkwell, F., and Eklundh, L.: Spatio-temporal patterns in vegetation start of season across the island of Ireland using the MERIS Global Vegetation Index, *ISPRS Journal of Photogrammetry and Remote Sensing*, 68, 79–94, doi:10.1016/j.isprsjprs.2012.01.004, 2012.
- PAN: PEP725 Pan European Phenology Data, online, <http://www.zamg.ac.at/pep725/>, 2011.
- Partanen, J., Koski, V., and Hanninen, H.: Effects of photoperiod and temperature on the timing of bud burst in Norway spruce (*Picea abies*), *Tree Physiol.*, 18, 811–816, 1998.
- Pääkkönen, E., Metsärinne, S., Holopainen, T., and Kärenlampi, L.: The ozone sensitivity of birch (*Betula pendula*) in relation to the developmental stage of leaves, *New Phytol.*, 132, 145–154, 1996.
- Penuelas, J., Rutishauser, T., and Filella, L.: Phenology feedbacks on climate change, *Science*, 324, 887–888, 2009.
- Pinto, C. A., Henriques, M. O., Figueiredo, J. P., David, J. S., Abreu, F. G., Pereira, J. S., Correia, I., and David, T. S.: Phenology and growth dynamics in Mediterranean evergreen oaks: Effects of environmental conditions and water relations, *Forest Ecol. Manag.*, 262, 500–508, doi:10.1016/j.foreco.2011.04.018, 2011.
- Polgar, C. A. and Primack, R. B.: Leaf-out phenology of temperate woody plants: from trees to ecosystems, *New Phytol.*, 191, 926–941, doi:10.1111/j.1469-8137.2011.03803.x, 2011.
- Rybski, D., Holsten, A., and Kropp, J. P.: Towards a unified characterization of phenological phases: Fluctuations and correlations with temperature, *Physica A-statistical Mechanics and Its Applications*, 390, 680–688, doi:10.1016/j.physa.2010.10.043, 2011.
- Scheel, H. E., Areskou, H., Geiss, H., Gomiscek, B., Granby, K., Haszpra, L., Klasinc, L., Kley, D., Laurila, T., Lindskog, A., Roemer, M., Schmitt, R., Simmonds, P., Solberg, S., and Toupance, G.: On the spatial distribution and seasonal variation of lower-troposphere ozone over Europe, *J. Atmos. Chem.*, 28, 11–28, 1997.
- Schurgers, G., Arneth, A., Holzinger, R., and Goldstein, A. H.: Process-based modelling of biogenic monoterpene emissions combining production and release from storage, *Atmos. Chem. Phys.*, 9, 3409–3423, doi:10.5194/acp-9-3409-2009, 2009.
- Siljamo, P., Sofiev, M., Ranta, H., Linkosalo, T., Kubin, E., Ahas, R., Genikhovich, E., Jatczak, K., Jato, V., Nekovar, J., Minin, A., Severova, E., and Shalaboda, V.: Representativeness of point-wise phenological *Betula* data collected in different parts of Europe, *Glob. Ecol. Biogeogr.*, 17, 489–502, doi:10.1111/j.1466-

- 8238.2008.00383.x, 2008.
- Simpson, D.: Biogenic emissions in Europe 2: Implications for ozone control strategies, *J. Geophys. Res.*, 100, 22891–22906, 1995.
- Simpson, D., Emberson, L., Ashmore, M. R., and Tuovinen, J. P.: A comparison of two different approaches for mapping potential ozone damage to vegetation. A model study, *Environ. Poll.*, 146, 715–725, 2007.
- Simpson, D., Winiwarer, W., Börjesson, G., Cinderby, S., Ferreira, A., Guenther, A., Hewitt, C. N., Janson, R., Khalil, M. A. K., Owen, S., Pierce, T. E., Puxbaum, H., Shearer, M., Skiba, U., Steinbrecher, R., Tarrasón, L., and Öquist, M. G.: Inventorying emissions from Nature in Europe, *J. Geophys. Res.*, 104, 8113–8152, 1999.
- Simpson, D., Butterbach-Bahl, K., Fagerli, H., Kesik, M., Skiba, U., and Tang, S.: Deposition and Emissions of Reactive Nitrogen over European Forests: A Modelling Study, *Atmos. Environ.*, 40, 5712–5726, doi:10.1016/j.atmosenv.2006.04.063, 2006.
- Simpson, D., Yttri, K., Klimont, Z., Kupiainen, K., Caseiro, A., Gelencsér, A., Pio, C., and Legrand, M.: Modeling Carbonaceous Aerosol over Europe. Analysis of the CARBOSOL and EMEP EC/OC campaigns, *J. Geophys. Res.*, 112, D23S14, doi:10.1029/2006JD008158, 2007.
- Simpson, D., Benedictow, A., Berge, H., Bergström, R., Emberson, L. D., Fagerli, H., Flechard, C. R., Hayman, G. D., Gauss, M., Jonson, J. E., Jenkin, M. E., Nyíri, A., Richter, C., Semeena, V. S., Tsyro, S., Tuovinen, J.-P., Valdebenito, Á., and Wind, P.: The EMEP MSC-W chemical transport model – technical description, *Atmos. Chem. Phys.*, 12, 7825–7865, doi:10.5194/acp-12-7825-2012, 2012.
- Simpson, D., Tuovinen, J. P., Emberson, L. D., and Ashmore, M. R.: Characteristics of an ozone deposition module, *Water Air Soil Pollut.: Focus*, 1, 253–262, 2001.
- Simpson, D., Tuovinen, J. P., Emberson, L. D., and Ashmore, M. R.: Characteristics of an ozone deposition module II: sensitivity analysis, *Water Air Soil Pollut.*, 143, 123–137, 2003.
- Sitch, S., Cox, P. M., Collins, W. J., and Huntingford, C.: Indirect radiative forcing of climate change through ozone effects on the land-carbon sink, *Nature*, 448, 791–795, 2007.
- Skamarock, W. C. and Klemp, J. B.: A time-split non-hydrostatic atmospheric model for weather research and forecasting applications, *J. Comp. Phys.*, 227, 3465–3485, doi:10.1016/j.jcp.2007.01.037, 2008.
- Skjøth, C. A., Geels, C., Hvidberg, M., Hertel, O., Brandt, J., Frohn, L. M., Hansen, K. M., Hedegaard, G. B., Christensen, J. H., and Moseholm, L.: An inventory of tree species in Europe – An essential data input for air pollution modelling, *Ecol. Modell.*, 217, 292–304, 2008.
- Skjøth, C. A., Geels, C., Berge, H., Gyldenkerne, S., Fagerli, H., Ellermann, T., Frohn, L. M., Christensen, J., Hansen, K. M., Hansen, K., and Hertel, O.: Spatial and temporal variations in ammonia emissions – a freely accessible model code for Europe, *Atmos. Chem. Phys.*, 11, 5221–5236, doi:10.5194/acp-11-5221-2011, 2011.
- Sliggers, S. and Kakebeeke, W. (Eds.): *Clearing the Air, 25 Years of the Convention on Long-Range Transboundary Air Pollution*, United Nations, Economic Commission for Europe, Geneva, <http://www.unece.org/env/lrtap>, 2004.
- Smith, B., Prentice, I. C., and Sykes, M. T.: Representation of vegetation dynamics in the modelling of terrestrial ecosystems: comparing two contrasting approaches within European climate space, *Global Ecol. Biogeogr.*, 10, 621–637, doi:10.1046/j.1466-822X.2001.t01-1-00256.x, 2001.
- Smith, B., Samuelsson, P., Wramneby, A., and Rummukainen, M.: A model of the coupled dynamics of climate, vegetation and terrestrial ecosystem biogeochemistry for regional applications, *Tellus A*, 63A, 87–106, doi:10.1111/j.1600-0870.2010.00477.x, 2011.
- Sofiev, M., Siljamo, P., Ranta, H., Linkosalo, T., Jaeger, S., Rasmussen, A., Rantio-Lehtimäki, A., Severova, E., and Kukkonen, J.: A numerical model of birch pollen emission and dispersion in the atmosphere. Description of the emission module, *Int. J. Biometeorol.*, 12, 1–14, doi:10.1007/s00484-012-0532-z, 2012.
- Sofiev, M. and Tuovinen, J.-P.: Factors determining the robustness of AOT40 and other ozone exposure indices, *Atmos. Environ.*, 35, 3521–3528, 2001.
- Steltzer, H. and Post, E.: Seasons and life cycles, *Science*, 324, 886–887, 2009.
- Sutton, M., Simpson, D., Levy, P., Smith, R., Reis, S., van Oijen, M., and de Vries, W.: Uncertainties in the relationship between atmospheric nitrogen deposition and forest carbon sequestration, *Glob. Change Biol.*, 14, 1–7, doi:10.1111/j.1365-2486.2008.01636.x, 2008.
- Sutton, M. A., Nemitz, E., Erisman, J. W., Beier, C., Butterbach-Bahl, K., Cellier, P., de Vries, W., Cotrufo, F., Skiba, U., Di Marco, C., Jones, S., Laville, P., Soussana, J. F., Loubet, B., Twigg, M., Famulari, D., Whitehead, J., Gallagher, M. W., Nefitel, A., Flechard, C. R., Herrmann, B., Calanca, P. L., Schjoerring, J. K., Daemmgen, U., Horvath, L., Tang, Y. S., Emmett, B. A., Tietema, A., Penuelas, J., Kesik, M., Brüeggemann, N., Pilegaard, K., Vesala, T., Campbell, C. L., Olesen, J. E., Dragosits, U., Theobald, M. R., Levy, P., Mobbs, D. C., Milne, R., Viovy, N., Vuichard, N., Smith, J. U., Smith, P., Bergamaschi, P., Fowler, D., and Reis, S.: Challenges in quantifying biosphere – atmosphere exchange of nitrogen species, *Environ. Poll.*, 150, 125–139, 2007.
- Sykes, M. T., Prentice, I. C., and Cramer, W.: A bioclimatic model for the potential distributions of north European tree species under present and future climates RID B-8221-2008, *J. Biogeogr.*, 23, 203–233, 1996.
- Tuovinen, J.-P., Emberson, L., and Simpson, D.: Modelling ozone fluxes to forests for risk assessment: status and prospects, *Annals of Forest Science*, 66, 401, doi:10.1051/forest/2009024, 2009.
- Tuovinen, J. P., Simpson, D., Ashmore, M. R., Emberson, L. D., and Gerosa, G.: Robustness of modelled ozone exposures and doses, *Environ. Poll.*, 146, 578–586, 2007.
- Tuovinen, J.-P., Ashmore, M., Emberson, L., and Simpson, D.: Testing and improving the EMEP ozone deposition module, *Atmos. Environ.*, 38, 2373–2385, 2004.
- Tuovinen, J.-P., Simpson, D., Mikkelsen, T., Emberson, L., M., M. R. A., Aurela, Cambridge, H. M., Hovmand, M. F., Jensen, N. O., Laurila, T., Pilegaard, K., and Ro-Poulsen, H.: Comparisons of measured and modelled ozone deposition to forests in Northern Europe, *Water, Air and Soil Pollution: Focus*, 1, 263–274, 2001.
- UNECE/WHO: *Modelling and Assessment of the Health Impact of Particulate Matter and Ozone*, United Nations Economic Commission for Europe, Geneva Switzerland, 2004.

- Vieno, M., Dore, A. J., Stevenson, D. S., Doherty, R., Heal, M. R., Reis, S., Hallsworth, S., Tarrason, L., Wind, P., Fowler, D., Simpson, D., and Sutton, M. A.: Modelling surface ozone during the 2003 heat-wave in the UK, *Atmos. Chem. Phys.*, 10, 7963–7978, doi:10.5194/acp-10-7963-2010, 2010.
- Villordon, A., LaBonte, D., and Firon, N.: Development of a simple thermal time method for describing the onset of morpho-anatomical features related to sweetpotato storage root formation, *Scientia Horticulturae*, 121, 374–377, doi:10.1016/j.scienta.2009.02.013, 2009.
- Wang, J. Y.: A critique of the heat unit approach to plant-response studies, *Ecology*, 41, 785–790, doi:10.2307/1931815, 1960.
- Wiedinmyer, C., Guenther, A., Harley, P., Hewitt, C., Geron, C., Artaxo, P., Steinbrecher, R., and Rasmussen, R.: Global organic emissions from vegetation, in: *Emissions of Atmospheric Trace Compounds*, edited by: Granier, C., Artaxo, P., and Reeves, C. E., 115–170, Kluwer Academic Publishers, 2004.
- Willmott, C. J.: Some comments on the evaluation of model performance, *B. Am. Meteorol. Soc.*, 63, 1309–1313, doi:10.1175/1520-0477(1982)063<1309:SCOTEO>2.0.CO;2, 1982.
- Wipfler, E. L., Metselaar, K., van Dam, J. C., Feddes, R. A., van Meijgaard, E., van Uft, L. H., van den Hurk, B., Zwart, S. J., and Bastiaanssen, W. G. M.: Seasonal evaluation of the land surface scheme HTESSEL against remote sensing derived energy fluxes of the Transdanubian region in Hungary, *Hydrol. Earth Syst. Sci.*, 15, 1257–1271, doi:10.5194/hess-15-1257-2011, 2011.
- Zhang, X., Friedl, M., Schaaf, C., and Strahler, A.: Climate controls on vegetation phenological patterns in northern mid- and high latitudes inferred from MODIS data, *Global Change Biol.*, 10, 1133–1145, doi:10.1111/j.1529-8817.2003.00784.x, 2004.
- Zhang, Y.: Online-coupled meteorology and chemistry models: history, current status, and outlook, *Atmos. Chem. Phys.*, 8, 2895–2932, doi:10.5194/acp-8-2895-2008, 2008.
- Ziello, C., Estrella, N., Kostova, M., Koch, E., and Menzel, A.: Influence of altitude on phenology of selected plant species in the Alpine region (1971–2000), *Clim. Res.*, 39, 227–234, doi:10.3354/cr00822, 2009.